Measurement of asymmetries in polarized $\gamma N \rightarrow \pi N$, with E_γ from 600 to 900 MeV*

G. Knies,† H. Oberlack,‡ A. Rittenberg, and A. H. Rosenfeld
Lawrence Berkeley Laboratory, University of California, Berkeley, California 94720

M. Bogdanski
Université de Neuchâtel, Neuchâtel, Switzerland

G. Smadja
Centre d'Études Nucléaires, Saclay, Gif-sur-Yvette, France
(Received 6 June 1974)

We report on the measurement of asymmetries in the single-pion photoproduction reactions $\gamma p \rightarrow n\pi^+$, $\gamma p \rightarrow p\pi^0$, and $\gamma n \rightarrow p\pi^-$, induced by linearly polarized photons of energies from 610 to 940 MeV. The experiment was carried out using the back-scattered laser beam and the 82-in. bubble chamber at SLAC. We compare the new data with predictions from a partial-wave analysis.

I. INTRODUCTION

In single-pion photoproduction, there is a great imbalance in the kind of data available. Cross-section measurements abound compared to asymmetries from linearly polarized photons, target asymmetries, and recoil-nucleon polarizations, with a frequency of approximately 3000 : 150 : 150 : 150 data points, respectively, for photon energies below 1.7 GeV. In an amplitude analysis of single-pion photoproduction there is a great need for more non-cross-section data for a better determination of γNN^* coupling strengths and for the removal of ambiguities in the partial-wave analysis.

We report here the measurement of 141 asymmetry data points, in a kinematic region where there were virtually no previous measurements. The breakdown into reactions was as follows.

(π^+): $\gamma p \rightarrow n\pi^+$ 55 data points;

(π^0): $\gamma p \rightarrow p\pi^0$ 41 data points;

(π^-): $\gamma n \rightarrow p\pi^-$ 45 data points.

II. EXPERIMENTAL PROCEDURE

A. The beam

The experiment used a back-scattered laser beam[1-3] with nearly 100% linear polarization. The 82-in. bubble chamber at SLAC was both the target and detector. There were four different beam settings for the hydrogen exposure, and two beam settings for the deuterium exposure. The peak energies and widths, path lengths, and number of useful events are given in Table I. The beam spectra were determined by counting pairs every 50th frame, and measuring a sample of pairs at each beam setting. With the known pair-production cross section,[4] we infer the intensity spectra, which are shown in terms of events/μb for each hydrogen run in Fig. 1.

B. Events from hydrogen

All film was scanned twice, and disagreements were resolved in a third scan. The events for reactions (π^+) and (π^0) are one-prong events. The bubble density allows for an unambiguous separation of protons from pions. We know the beam direction precisely, but its energy full width is 40–60 MeV, so for the kinematic reconstruction we may either (1) use all the beam information and make a one-constraint ($1c$) fit, or (2) not constrain the beam energy and then make a $0c$ calculation. (Constraint for some events is not very useful and only biases the fit.) Events with an additional (invisible) π^0 are clearly separated from the single-pion production on kinematic grounds. When such two-pion events are mistaken as single-pion events, the resulting $0c$-calculated beam energy is well outside (below) the beam spectrum. This feature has been checked with two-pion events from the reaction $\gamma p \rightarrow p\pi^+\pi^-$, which are observed as three-prong events in this same experiment, by treating them kinematically as one-prong events in the following way:

$$\gamma p \rightarrow p(\pi^+ + \pi^-) \text{ as } p\pi^0,$$
$$\gamma p \rightarrow \pi^+(p + \pi^-) \text{ as } \pi^+ n,$$
$$\gamma p \rightarrow \pi^-(p + \pi^+) \text{ as } \pi^- n.$$

The energy from the $0c$ kinematic solution for these wrong $N\pi$ hypotheses was well below the true beam spectrum.

The combined scanning efficiency of the two scans for one-prong events was better than 99%. The scanning efficiency was independent of the

TABLE I. Characteristics of our six runs, and event yields.

Run No.	$E_{\gamma,\text{peak}}$ (MeV)	ΔE_γ FWHM (MeV)	Total flux (events/μb)	Target	Number of events used for asymmetries $n\pi^+$	$p\pi^0$
1	715	40	55.1	Hydrogen	5912	1986
2	745	35	30.3	Hydrogen	2745	1226
3	770	40	52.4	Hydrogen	4200	2287
4	904	60	51.0	Hydrogen	2584	1546
5	763	50	51.0	Deuterium	$p\pi^-(p_{\text{spect}}<150$ MeV/$c)$	
6	726	45	46.7	Deuterium	5225	

beam energy and the angle ϕ used in the asymmetry calculation, where ϕ is the angle between the direction of the γ polarization and the normal to the production plane.

In Tables II and III we shall present asymmetries using (a) all events (fitted as 1c), and (b) only those events having well-determined 0c fits. We now briefly discuss these two sets of events.

First, all events were fitted 1c with E_γ approximated as a Gaussian of half-width δE_γ; while this has the advantage of allowing asymmetries to be measured at all angles and of treating all events uniformly, it has the undesired effect of biasing each individual event's beam energy E_γ^i toward the central value E_γ. Hence in Tables II(a) and III(a) we can safely present events only in wide energy bins, corresponding to an entire run.

Next, we took advantage of the good energy resolution available from the measurement of events with long tracks ($\gamma p \to n\pi^+$ with $\theta^*_{\gamma,\pi} < 60°$ and $\gamma p \to p\pi^0$ with $\theta^*_{\gamma,\pi} > 120°$); to avoid the bias mentioned above, each such event was 0c-calculated, with the beam information ignored. Thus, for these well-measured events in selected angular regions, we may present asymmetries with a finer (30-MeV) energy binning than above; this is done in Tables II(b) and III(b). There are, however, two problems related to these events where E_γ is determined entirely by direct measurement, and δE_γ varies with azimuth angle:

(1) In earlier experiments with this same polarized beam, we frequently flipped the direction of polarization of the photons from vertical to horizontal, but when we scanned the film we found that the scanning efficiency was independent of azimuth, so we mistakenly stopped flipping the polarization. What we forgot was that the energy uncertainty δE_γ for one-prong events is worst for the events with a vertical production plane, so they are smeared out into a broader range of E_γ than their horizontally produced companions. If not corrected for, this effect will introduce apparent asymmetries.

(2) Since we are using center-of-mass production angles θ^* ($\equiv\theta^*_{\gamma,\pi}$) rather than the directly measured laboratory production angles θ, the uncertainty in the (calculated) beam energy smears the θ^* distribution via the Lorentz transformation. We have chosen an energy and θ^* binning so that both effects produce changes in the number of events per ΔE-$\Delta\theta^*$ bin of not more than 30% in the worst cases. In addition to protecting against bias by choosing unusually large energy bins, we have performed an unfolding of the smearing of the measured distribution due to the measurement errors and thereby actually corrected the bias.[5]

C. Events from deuterium

We follow the standard procedures of selecting three-prong and two-prong events with a slow proton ($\gamma d \to p_s p\pi^-$, $p_s < 150$ MeV/c) and then using the spectator model (Fig. 2) to express these as γn

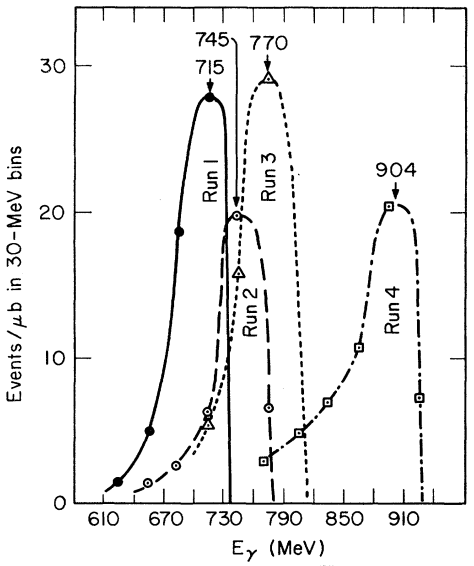

FIG. 1. Path-length distribution for each of our four hydrogen runs. The symbols are plotted in the middle of the 30-MeV bins to which they refer. The curves do not reproduce the actual spectra, but merely join the symbols.

TABLE II. (a) Asymmetries in $\gamma p \to n\pi^+$ from 1*c* solutions. (b) Asymmetries in $\gamma p \to n\pi^+$ from well-determined 0*c* events. θ^* is the c.m. angle between the photon and pion; E_γ is the average lab photon energy of events from each run; N is the number of events in each run (same numbers as in Table I).

(a)

E_γ (MeV) \ θ^* (deg)	10	30	50	70	90	110	130	150	170
700 (N=5912)	0.36±0.08	0.88±0.04	0.76±0.04	0.69±0.03	0.66±0.04	0.60±0.05	0.46±0.06	0.33±0.09	0.10±0.17
737 (N=2745)	0.45±0.12	0.88±0.06	0.74±0.05	0.72±0.05	0.54±0.06	0.48±0.07	0.47±0.09	0.29±0.12	0.10±0.21
762 (N=4200)	0.49±0.10	0.88±0.05	0.71±0.04	0.51±0.05	0.44±0.05	0.50±0.05	0.53±0.07	0.21±0.10	-0.13±0.25
885 (N=2584)	0.46±0.12	0.81±0.06	0.62±0.06	0.41±0.07	-0.04±0.08	-0.07±0.08	0.00±0.09	-0.02±0.12	0.00±0.20

(b)

E_γ (MeV) \ θ^* (deg)	10	30	50	Number of 0*c* events	
610–640	0.24±0.31	1.21±0.20	0.90±0.13	90	
640–670	0.28±0.18	0.90±0.10	0.78±0.09	307	Data
670–700	0.33±0.15	0.85±0.07	0.75±0.06	799	from
700–730	0.48±0.09	0.91±0.05	0.79±0.04	1387	runs
730–760	0.56±0.11	0.95±0.06	0.70±0.06	919	1-3
760–790	0.56±0.14	0.79±0.07	0.59±0.07	664	
790–820	0.22±0.32	0.73±0.19	0.72±0.20	129	Data
820–880	0.00±0.20	1.07±0.09	0.74±0.11	319	from
880–940	0.72±0.14	0.94±0.08	0.61±0.08	600	run 4

TABLE III. (a) Asymmetries in $\gamma p \to p\pi^0$, from 1*c* solutions. (b) Asymmetries in $\gamma p \to p\pi^0$ from well-determined 0*c* events. θ^*, E_γ, and N are defined in the Table II caption.

(a)

E_γ (MeV) \ θ^* (deg)	10	30	50	70	90	110	130	150	170
700 (N=1986)	···	0.42±0.13	0.60±0.08	0.84±0.06	0.85±0.05	0.85±0.06	0.78±0.09	0.35±0.14	−0.02±0.23
737 (N=1226)	···	0.26±0.21	0.89±0.09	0.77±0.07	0.85±0.07	0.73±0.08	0.72±0.11	0.33±0.15	0.35±0.33
762 (N=2287)	···	0.53±0.13	0.62±0.08	0.83±0.05	0.68±0.05	0.69±0.06	0.63±0.08	0.22±0.12	0.21±0.23
885 (N=1546)	···	0.34±0.16	0.46±0.10	0.47±0.07	0.45±0.07	0.32±0.07	0.44±0.09	0.34±0.12	0.55±0.21

(b)

E_γ (MeV) \ θ^* (deg)	130	150	170	Number of 0*c* events	
610–640	1.33±0.35	···	···	12	
640–670	0.94±0.22	−0.32±0.30	···	56	Data
670–700	0.82±0.14	0.22±0.21	···	127	from
700–730	0.76±0.10	0.31±0.16	···	237	runs
730–760	0.60±0.10	0.50±0.15	···	260	1-3
760–790	0.48±0.12	0.17±0.18	···	214	
790–820	0.94±0.20	0.42±0.36	···	50	Data
820–880	0.33±0.18	0.44±0.17	0.56±0.30	140	from
880–940	0.27±0.13	0.21±0.18	0.74±0.32	195	run 4

$\to p\pi^-$. First we checked experimentally on the validity of the model and the possible presence of "deuteron effects" such as (a) dynamical effects of the off-shell nature of the target neutron, (b) interference effects between the two production amplitudes of Fig. 2 [the spectator model considers only diagram 2(a)], (c) the Pauli principle, and (d) final-state interactions.

From the familiar ideas of Chew-Low pole extrapolation,[6] it is clear that both inadequacies of the spectator model and off-mass-shell effects decrease for small spectator momentum. We have therefore compared asymmetries determined from that half of the events with $p_s < 50$ MeV/c with asymmetries from the other half ($50 < p_s < 150$ MeV/c). Within statistics they agreed, with no systematic trend visible. We conclude that our procedures are valid within the statistical accuracy quoted.

The data processing was the same as for the hydrogen events with the following exceptions: Without using the beam energy information we have 3c fits, and the fitted energy resolution δE_γ (typically ≈ 15 MeV) is better than the beam width. Therefore, we do not use the beam information, but rely on the unbiased 3c fits. We present these data in 40-MeV energy bins of effective lab photon energy.

Just as for proton events, the combined scanning efficiency is better than 99% and is independent of ϕ.

There is one final possible difficulty, which we shall now show is small. The photon polarization is given in the laboratory system, but the asymmetry measurement is done in a frame of reference that is moving. If α is the angle between the photon beam direction as seen in the lab system and the photon beam direction as seen in the γ-n c.m. system, the depolarization of the photons in the γ-n c.m. system is not larger than $1 - \cos^2\alpha$. The average value of $1 - \cos^2\alpha$ in the events used was $\langle 1 - \cos^2\alpha \rangle = 0.0024 \pm 0.0028$, and the depolarization effect, therefore, is negligible.

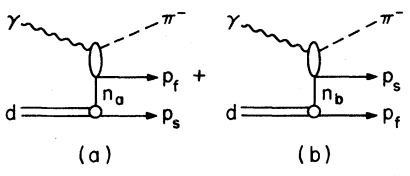

FIG. 2. Impulse-approximation diagrams for $\gamma d \to pp\pi^-$. The slower proton (in the lab) is labeled p_s; the faster, p_f. The spectator model ignores diagram (b).

TABLE IV. Asymmetries in $\gamma n \to p\pi^-$. 7427 3c fits were obtained, but the asymmetries are calculated for the 5225 of them which had a spectator momentum of < 150 MeV/c. θ^* and N are defined in the Table II caption. E_γ is not the real photon energy, but the effective lab energy for the reaction $\gamma n \to p\pi^-$.

E_γ (MeV) \ θ^* (deg)	10	30	50	70	90	110	130	150	170
610–650 ($N = 392$)	0.43 ± 0.32	0.68 ± 0.18	0.56 ± 0.18	0.77 ± 0.15	0.47 ± 0.22	0.30 ± 0.19	0.26 ± 0.22	0.04 ± 0.26	−0.95 ± 0.36
650–690 ($N = 946$)	0.15 ± 0.23	0.81 ± 0.11	0.85 ± 0.10	0.57 ± 0.10	0.18 ± 0.11	0.27 ± 0.12	−0.25 ± 0.14	−0.09 ± 0.13	0.00 ± 0.24
690–730 ($N = 1768$)	−0.12 ± 0.16	0.57 ± 0.08	0.54 ± 0.08	0.31 ± 0.07	0.08 ± 0.08	−0.01 ± 0.09	−0.26 ± 0.10	−0.01 ± 0.10	−0.07 ± 0.16
730–770 ($N = 1698$)	−0.32 ± 0.17	0.47 ± 0.09	0.45 ± 0.08	0.27 ± 0.08	−0.28 ± 0.09	−0.04 ± 0.10	−0.08 ± 0.11	0.04 ± 0.10	0.14 ± 0.15
770–810 ($N = 421$)	0.40 ± 0.31	0.19 ± 0.16	0.23 ± 0.17	−0.13 ± 0.18	−0.24 ± 0.18	−0.28 ± 0.22	−0.14 ± 0.18	−0.32 ± 0.20	−0.06 ± 0.33

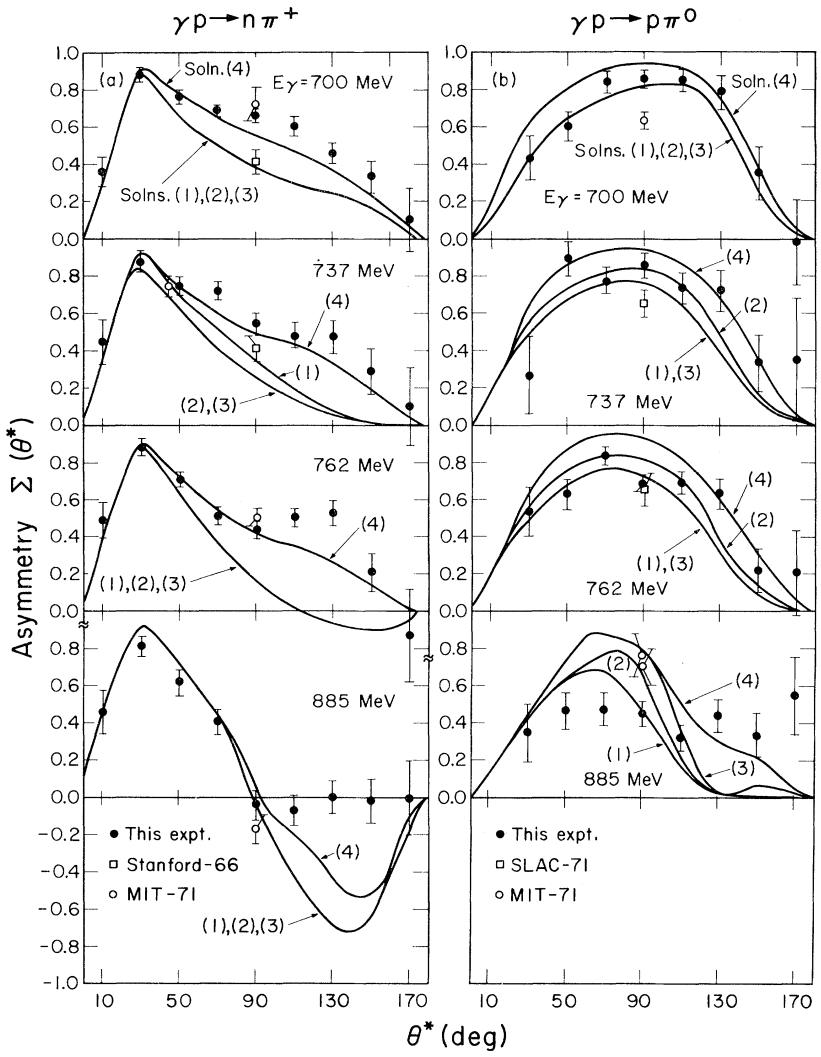

FIG. 3. Asymmetries for (a) $\gamma p \to n\pi^+$ and (b) $\gamma p \to p\pi^0$, at four beam energies. θ^* is the c.m. angle between the photon and the pion. The curves show the four solutions of KMO, Ref. 10. The solutions are indicated by parenthetical numbers.

III. RESULTS

The asymmetry is defined as

$$\Sigma(\theta^*) = \frac{d\sigma^{\perp} - d\sigma^{\parallel}}{d\sigma^{\perp} + d\sigma^{\parallel}}, \tag{1}$$

where $\perp$ ($\parallel$) means polarization vector perpendicular (parallel) to the production plane, and θ^* is the c.m. angle between the photon and the pion. $\Sigma(\theta^*)$ is related to the double-differential cross section via

$$\frac{d^2\sigma}{d\phi\, d\cos\theta^*} = \frac{1}{\pi}\frac{d\sigma}{d\cos\theta^*}[1 + \Sigma(\theta^*)\cos 2\phi], \tag{2}$$

where ϕ is the angle between the normal to the production plane and the direction of the polarization. Since our experiment has a uniform acceptance over the full ϕ range, we determine the asymmetry merely by forming the moment $\langle \cos 2\phi \rangle$ in Eq. (2). We have done this for various E-θ^* intervals. As a check on systematic biases we also formed the moments $\langle \cos\phi \rangle$, $\langle \sin\phi \rangle$, and $\langle \sin 2\phi \rangle$, which must be zero. The distributions of the experimental ratios $\langle \cos\phi \rangle / \delta\langle \cos\phi \rangle$, $\langle \sin\theta \rangle / \delta\langle \sin\phi \rangle$, and $\langle \sin 2\phi \rangle / \delta\langle \sin 2\phi \rangle$ are, in fact, compatible with a normal distribution $N(0, 1)$.

In Tables II, III, and IV, and in Figs. 3(a), 3(b), and 4, we show the asymmetries for the reactions (π^+), (π^0), and (π^-), respectively. The asymmetries show very significant dependences on the energy and the production angle.

There are a few earlier asymmetry measurements[7-9] in the same kinematic region, also shown in Figs. 3, 4. There are no disagreements between those experiments and our experiment.

IV. COMPARISON WITH PARTIAL-WAVE ANALYSIS

Figures 3 and 4 compare our results with the predictions of the partial-wave analysis of Knies, Moorhouse, and Oberlack (KMO).[10] Also included in the figures are the few data points (14 in all, compared with our 141) labeled Stanford-66,[7] MIT-71,[8] and SLAC-71,[9] which were available to KMO. We note the following:

(1) In the $n\pi^+$ asymmetries the old KMO solutions (1), (2), and (3) are qualitatively in disagreement with the data of all four energies. They fail to predict a shoulder at $\theta^* \approx 130°$ for E_γ in the range from 700 to 762 MeV; also, the predicted dip at $\theta^* = 130°$ for $E_\gamma = 885$ MeV is not observed in the data. Only solution (4) predicts the shoulder qualitatively correctly. However, at 885 MeV, it also predicts a dip at $\theta^* = 130°$, in disagreement with the data.

(2) In the $p\pi^0$ asymmetries, at $E_\gamma = 700$, 737, and 762 MeV, the predictions are quantitatively confirmed by our new data. At $E_\gamma = 885$ MeV, however, all four solutions show much more angular dependence than do the data, and are qualitatively wrong.

(3) In the $p\pi^-$ asymmetries, which are measured at energies from 610 to 810 MeV, the data beautifully confirm the qualitative features commonly predicted by all four solutions, namely a transition from positive to negative asymmetries as the energy increases. Note that these fits are almost "unaided" predictions—only three data points were previously available in the entire kinematic region covered by Fig. 4.

We conclude that in the energy range from 600 to 800 MeV, solution (4) of KMO predicts qualitatively the asymmetries we find for all three reactions, but that at $E_\gamma = 885$ MeV ($\sqrt{s} \approx 1600$ MeV) all four KMO solutions disagree with both of the γp reactions. We are now repeating[11] the partial-wave analysis of KMO, using our new data.

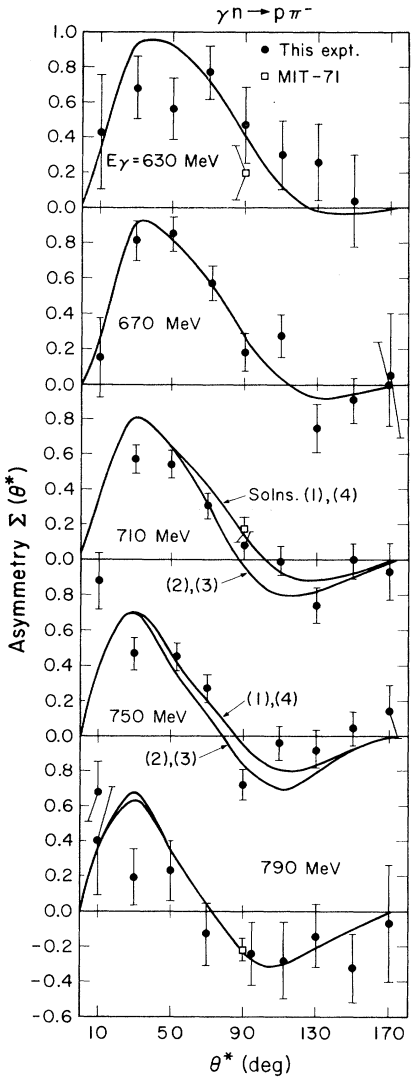

FIG. 4. Asymmetries for $\gamma n \to p\pi^-$, at five beam energies. θ^* is the c.m. angle between the photon and the pion. The curves show the four solutions of KMO, Ref. 10. The solutions are indicated by parenthetical numbers.

ACKNOWLEDGMENTS

We appreciate the support we received at various stages of this experiment from R. Gearhart, R. G. Moorhouse, J. J. Murray, M. S. Rabin, E. E. Ronat, and C. K. Sinclair. We gratefully acknowledge the work of Judy Bonnett, Wally Hendricks, Don Hirabayashi, and Joel Wissmar during the scanning and measuring phase of this experiment.

---

*This work was done under the auspices of the U. S. Atomic Energy Commission.

†Present address: Deutsches Elektronen Synchrotron, Hamburg, Germany.

‡Present address: Max-Planck-Institut für Physik und Astrophysik, 8 München 23, Germany.

[1]C. K. Sinclair *et al.*, IEEE Trans. Nucl. Sci. 16, 1065 (1969).

[2]J. Ballam *et al.*, Phys. Rev. D 5, 545 (1972).

[3]W. J. Podolsky, Ph.D. thesis, LBL Report No. UCRL-20128, 1971 (unpublished).

[4]T. M. Knasel, DESY Report No. 70/3, 1970 (unpublished).

[5]G. Knies, LBL Group A Physics Note 778, 1974 (unpub-

lished).
[6]G. F. Chew and F. E. Low, Phys. Rev. 113, 1640 (1959).
[7]F. F. Liu and S. Vitale, Phys. Rev. 144, 1093 (1966).
[8]J. Alspector *et al.*, Phys. Rev. Lett. 28, 1403 (1972).
[9]R. W. Zdarko and E. B. Dally, Nuovo Cimento 10A, 10 (1972).
[10]G. Knies, R. G. Moorhouse, and H. Oberlack, Phys. Rev. D 9, 2680 (1974).
[11]G. Knies, R. G. Moorhouse, H. Oberlack, and A. H. Rosenfeld, LBL Report No. LBL-2673, 1974 (unpublished).